Original Article

Smoke analysis of a new surgical system that applies low-temperature plasma

Boya Zhang[1,2], Qingyu Guan[1,2], Yunsheng Zhu[2], Jingjin Zhu[1,2], Xiaohan Liu[1,2], Shuaiqi Li[1,2], Rungong Yang[3], Xiru Li[2]

[1]School of Medicine, Nankai University, Tianjin, China; [2]Department of General Surgery, Chinese People's Liberation Army General Hospital, Beijing, China; [3]Department of Tissue Repair and Regeneration, Chinese People's Liberation Army General Hospital, Beijing, China

Contributions: (I) Conception and design: X Li, R Yang; (II) Administrative support: X Li, R Yang; (III) Provision of study materials or patients: X Li, R Yang; (IV) Collection and assembly of data: All authors; (V) Data analysis and interpretation: All authors; (VI) Manuscript writing: All authors; (VII) Final approval of manuscript: All authors.

Correspondence to: Xiru Li. Department of General Surgery, Chinese People's Liberation Army General Hospital, Beijing 100853, China. Email: 2468li@sina.com; Rungong Yang. Department of Tissue Repair and Regeneration, Chinese People's Liberation Army General Hospital, Beijing 100853, China. Email: yangrungong@139.com.

Background: The high-frequency electrotome (ES), which is widely used in surgical procedures, generates surgical smoke that is potentially hazardous to operating personnel. Previous research shows that the PlasmaBlade (PB) may be able to overcome this problem. The present study set out to analyze potentially hazardous surgical smoke generated during electrosurgery by the ES, the PB, and. a new surgical system that applies low-temperature plasma, the NTS-100.

Methods: *In vitro* and *in vivo* healthy porcine models were used to compare volatile organic compounds (VOCs) and particulate matter (PM) in smoke generated by the NTS-100, the PB, and the conventional ES when cutting liver, muscle, and skin and subcutaneous tissues. The detected indexes included the VOCs in surgical smoke, the concentration and percentage of each part, the PM2.5 concentration, the mass of particles, and the diameter distribution of particles.

Results: The smoke generated by the NTS-100 contained fewer hazardous components than that generated by the ES ($P<0.05$) and a comparable amount to that generated by the PB ($P>0.05$). The PM2.5 concentration and mass of particles in the smoke generated by the NTS-100 were lower than those with the ES ($P<0.05$ and $P<0.01$, respectively) and similar to those with the PB ($P>0.05$). The NTS-100 generated larger particles than did the ES and the PB ($P<0.05$).

Conclusions: Surgical smoke contains harmful VOCs and PM, but the NTS-100 generated less hazardous surgical smoke than did the conventional ES and performed comparably to the PB. Therefore, using the NTS-100 may reduce the potential hazard of surgical smoke to operating room personnel.

Keywords: High-frequency electrotome; low-temperature plasma; PlasmaBlade (PB); surgical smoke

Submitted Jan 31, 2022. Accepted for publication Jul 04, 2022.
doi: 10.21037/atm-22-608
View this article at: https://dx.doi.org/10.21037/atm-22-608

Introduction

Surgical smoke has become a concern during the COVID-19 pandemic, despite the lack of convincing evidence that it can transmit the SARS-CoV-2 virus (1,2). However, surgical smoke is known to contain volatile organic compounds (VOCs) and particulate matter (PM) (3), making it an occupational hazard for developing chronic obstructive pulmonary disease as well as damage to the respiratory, circulatory, and neurological systems (3). Furthermore, from a practical perspective, a large amount of surgical smoke can obscure the operators' view, prolonging the surgical procedure.

Figure 1 New surgical system that applies low-temperature plasma (NTS-100) and its electrode.

The high-frequency electrotome (ES), which is commonly used in operations, can generate a large amount of surgical smoke. To remedy this problem, the PlasmaBlade (PB) was developed. The PB works by delivering brief (40-μs range), high-frequency pulses of radiofrequency energy along the edge of a 12.5-μm-thin, insulated electrode (4). Unlike the ES, which typically operates in the range of 200–350 ℃ (4), the PB operates in the range of 40–170 ℃ and thus uses less energy to attain a lower temperature while reducing the amount of surgical smoke (5). A new surgical system which applies low-temperature plasma, the NTS-100, has also been developed (*Figure 1*). It also uses pulsed radiofrequency energy to improve the high-frequency generator and enhance the frequency of the main engine. The surface temperature of the NTS-100 is ~70 ℃; in comparison, that of the PB is ~80 ℃ (5). The NTS-100 also produces less surgical smoke than the ES.

This study aimed to analyze surgical smoke generated by the conventional ES, the PB, and the NTS-100 during electrosurgery. To do this, *in vitro* and *in vivo* porcine models were used due to the genetic sequence similarity of pigs to humans. We present the following article in accordance with the ARRIVE reporting checklist (available at https://atm.amegroups.com/article/view/10.21037/atm-22-608/rc).

Methods

Materials

In vitro experiment

The *in vitro* experiment was conducted on a piece of porcine skin and subcutaneous tissue (approx. 7×12 cm), a piece of porcine muscle tissue (approx. 7×12 cm), and a piece of porcine liver tissue (approx. 6×12 cm), which were all determined to have a homogeneous cortex, a normal anatomical shape, and a smooth surface free of lesion or injury.

In vivo experiment

The *in vivo* study was conducted on three healthy male Bama mini-pigs (aged 10–13 months, weighing 37–40 kg), all of which came from the same breeding base, and were quarantined and qualified. The pigs had white skin on the back without spots or scars, were free of any animal or infectious diseases, and had been kept in a laboratory pen for 2 months before the experiment without any abnormalities. Bama mini-swine were chosen for this study due to having a similar genetic sequence, highly similar tissue organs and biochemical indicators (6), and few differences in the thickness and composition of each skin layer (7) compared to humans.

The experimental animals were provided by Beijing Shichuangshiji Miniature Pig Breeding Base (SCXK [Beijing] 2013-0008) and were bred in the Animal Experiment Center of the First Medical Center of the Chinese PLA General Hospital. The animal experiments were performed under a project license (No. 20160010703) granted by the Ethics Committee of Chinese PLA General Hospital. All animal experiments complied with the National Institutes of Health Guide for the Care and Use of Laboratory Animals.

Dissection strategy

Three different electrocautery devices were used in this study: the NTS-100, the comparative PB, and the conventional ES. The NTS-100 and PB were both on cut 6 mode and the conventional ES was on cut 45 mode; these are the most typical modes used during surgery. Smoke evacuation was not used during the experiment.

In vitro experiment

Each incision was controlled at 1-cm intervals and a constant velocity of 1-cm/s, to a length of 3 cm with a 0.5-cm cutting depth. When measuring the mean PM2.5 concentration, one incision was made at a time, but when measuring particle diameters, 20 incisions were made at a time. For all other indices detected, 10 incisions were made at a time.

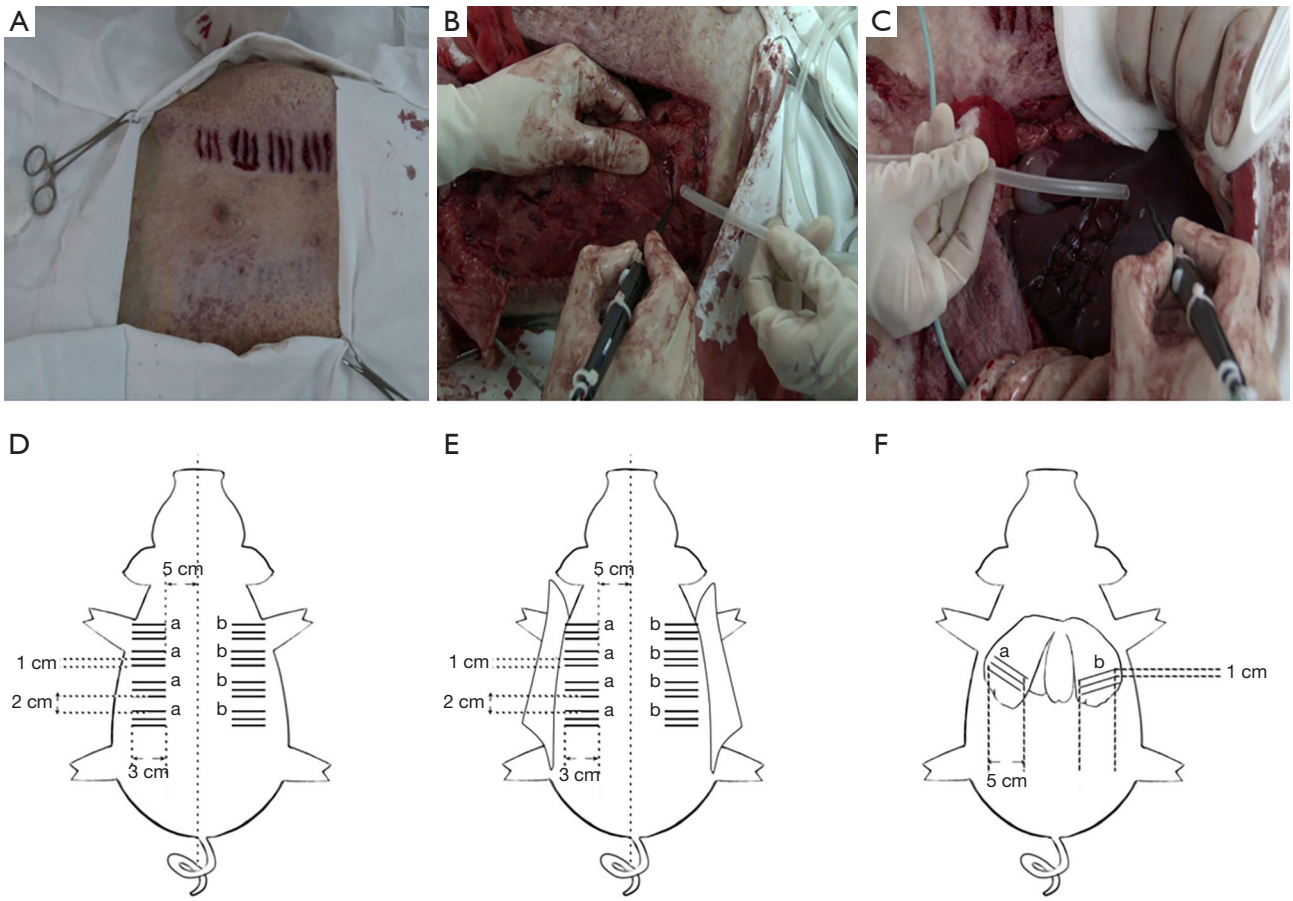

Figure 2 Incision design of *in vivo* experiment. (A) Incision of skin and subcutaneous; (B) incision of muscle; (C) incision of liver. (D) Incision design of skin and subcutaneous; (E) incision design of muscle; (F) incision design of liver. a, PEN site; b, PM2.5 sensor sampling site. PEN, portable electronic nose.

In vivo experiment

Figure 2 illustrates the incision designs for the liver, skin, and muscle tissue. For swine skin and subcutaneous tissues, relatively flat smooth skin was selected and three transverse incisions with a length of 3 cm and a 0.5-cm cutting depth were made at 1-cm intervals. For swine muscle tissues, the deep thoracic, subthoracic serratus, and external oblique abdominal muscle tissues were selected, and a total of three transverse incisions with a length of 3 cm and a 0.5-cm cutting depth were made at 1-cm intervals. For swine liver tissues, the larger left and right lobes of the liver were selected. Due to the abundant blood supply to the liver, it was difficult to achieve hemostasis in the electric cutting mode. Therefore, one transverse incision of 5 cm in length and 0.5 cm in depth was made near the distal end of the liver lobe.

Surgical smoke analysis

In vitro experiment

Figure 3 shows the fully closed surgical analysis system that we specially designed to collect as much surgical smoke as possible. First, experimental tissues were placed in a closed container. The negative plate was then tightly bonded to the tissues, and the lead from the negative plate was threaded through the adhesive plug and sealed. The electrosurgical surface was threaded through the other hole into the glue plug, and its length was tested (to the extent that the surface could penetrate the tissue by 0.5 cm). Next, the gas collection outlet was used to connect the helium supply to the closed container, and the enclosed container was continuously filled with helium gas at a controlled flow rate of 5 mL/min for a total of 3 mins until the original air inside

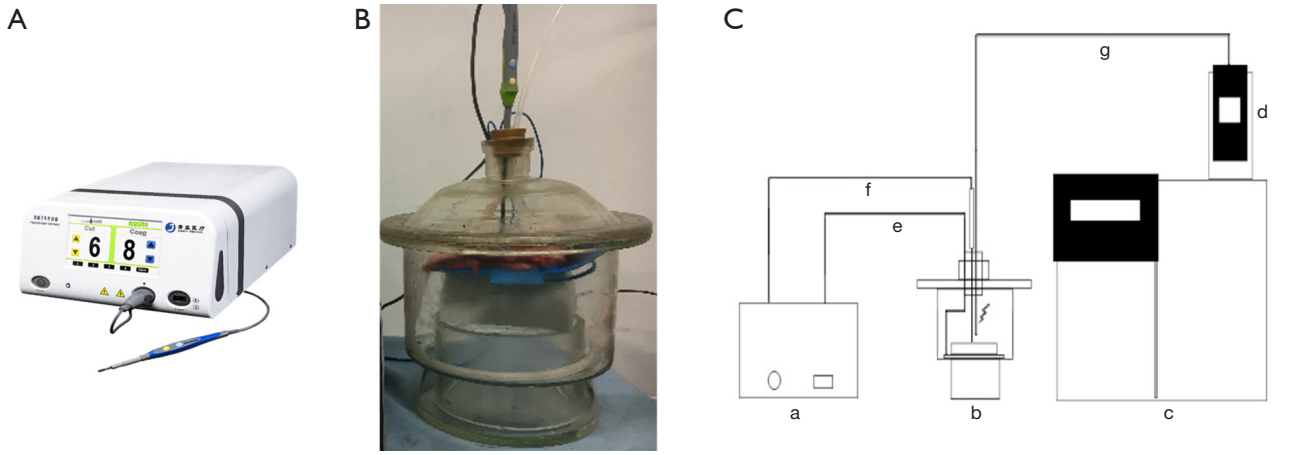

Figure 3 Experimental settings for *in vitro* experiments. (A) Surgical device (e.g., the new surgical system that applies low-temperature plasma) used in *in vitro* experiment. (B) Layout of surgical analysis system. (C) Plan view of the experimental setting. a, electrosurgical equipment main unit; b, closed container; c, GC-MS; d, TD instrument; e, negative electrode plate wiring; f, electrosurgical equipment wiring; g, gas transportation wiring. GC-MS, gas chromatography-mass spectrometry; TD, thermal desorption.

the enclosed container was exhausted. Then, as described above, 10 incisions were made with each of the ES, PB and NTS-100, after which a pump was used to move the newly generated smoke into thermal desorber (TD) tubes and empty air collection bottles. After any remaining smoke had been cleared, the same steps were performed as before. The collection bottles were filled with ultrapure water. Next, the PM2.5 sensor was put into the sealed container, and analysis was conducted before and after cutting one incision using the ES, PB, and NTS-100.

Measurement of VOCs with portable electronic nose

The assembly of the analysis system, evacuation of existing gas, and tissue dissection were performed as described above, and 10 parallel incisions 1 cm apart, 3 cm long, and 0.5 cm deep were made with the ES, PB, and NTS-100 to the tissues at 1 cm/s. The surgical smoke was collected using a pump for 1 min, the gas collection bottle was connected to the sample tube, and the PEN3 air sensor (Beijing Ying Sheng Heng Tai Technology Co., China) was applied to detect the gas composition and store the images.

VOCs analysis with gas chromatography–mass spectrometry

The assembly of the analysis system, evacuation of existing gas, and tissue dissection were performed in the same way as for the PEN3 analysis. After the parameters of the TD (7667A Thermal Desorber, Agilent, USA.) were set, the surgical smoke was collected by the gas sample tube into the TD tube for sampling and concentration for 5 min. At the completion of sampling, the TD was switched to dry-blowing mode to remove the original ambient components; the TD was heated up and the surgical smoke was vaporized under a high temperature and released into the gas chromatography–mass spectrometer (GC-MS; 5975T LTM-GC/MSD, Agilent, USA) for gas analysis.

Mean PM2.5 concentration

The PM2.5 sensor (LB-HD08, Lianyungang Arbor Electronics Technology Co.) was placed 5 cm from the tissue incisions in a sealed glass container. The assembly of the analysis system and evacuation of existing gas were performed in the same way as for the PEN3 analysis. The ES, PB, and NTS-100 were applied to tissues at 1 cm/s, and 10 parallel incisions 1 cm apart, 3 cm long, and 0.5 cm deep were made. The PM2.5 data were recorded before cutting (p1) and at 1 min after cutting (p2). The PM2.5 concentration was calculated as (p) = p2 – p1.

Diameter distribution of particles

The assembly of the analysis system and evacuation of existing gas were performed in the same way as for the PEN3 analysis. The ES, PB, and NTS-100 were applied to tissues at 1 cm/s, and incisions 1 cm apart, 3 cm long, and 0.5 cm deep were made. The surgical smoke was collected in a gas collection bottle containing 40 mL of ultrapure water (ELGA PURELAB Pulse, Elgar Ltd., UK) for 10 min using an air pump. The diameter distribution of particles was measured with a laser particle size analyzer (LPSA; Microtrac S3500, US Magitek Co.; range, 0.02–2,800 μm),

and each group of data was measured five times in total and the average value was taken.

Particle mass measurement

The assembly of the analysis system, evacuation of existing gas, and tissue dissection were performed the same as for the PEN3 analysis. After 24 h of equilibration under equilibrium conditions (30 ℃, 45–55% humidity), clean microporous membrane filters (pore size 0.45 μm; Beijing Beihua Liming Membrane Separation Technology Co., China) were placed in a constant temperature and humidity cabinet, and weighed by a parts per million microbalance (XP6, Mettler Toledo GmbH, Zurich, Switzerland). Each filter membrane was weighed more than 10 times; the highest and lowest values were excluded, and the average value of each filter membrane was the original mass of the membrane, which was recorded as m1. After 10 min of sampling with the gas collection pump, the microporous membrane filters with the filtered particles were removed and equilibrated in a constant temperature and humidity chamber for 24 h. They were weighed more than 10 times, the highest and lowest values were excluded, and the average mass of each filter membrane was recorded as m2. This process was repeated three times and the average was taken. The mass of a particle (m) = m2 – m1.

***In vivo* experiment**

The Bama pigs were anesthetized by intramuscular injection of ketamine hydrochloride and tamsulosin II (0.4 mL/kg) behind the neck, and then we made median abdominal incisions and cut the skin layer by layer to expose the target organs. The next step was to make incisions using the ES, PB, and NTS-100, successively. Finally, an air collection pump was used to collect the newly produced smoke in the gas collection bottle. All the experimental animals were euthanized after this research.

VOCs measurement with PEN3

The gas collection pump outlet was connected to the gas collection bottle with a rubber tube, and the suction port was connected to another rubber tube. The rubber tube for gas collection was tightly attached to the scalpel tip so that they moved in line during electrosurgery. Surgical smoke was collected until the end of the cutting procedure, at which point the rubber tube was disconnected from the gas collection bottle and the bottle stopper was tightened. Then, the inlet tube of the gas collection bottle and the PEN3 were connected to a computer to display the change in gas composition detected by each probe within 2 min, and the images were stored.

Real-time concentration of PM2.5

The PM2.5 sensor was placed at a fixed vertical distance of 5 cm above the incisions to measure the real-time PM2.5 concentration when the tissue was cut at the beginning of surgery.

Analytical equipment

TD and GC-MS

Gas analysis in this experiment used a GC-MS linked to a TD tube. A temperature-dependent variation in affinity exists between the mobile and stationary phases of gas chromatography, which allows for sequential separation and analysis of a wide range of VOCs (8). The procedure conducted in this study was as follows: the temperature was maintained at 25 ℃ for 5 min, increased to 80 ℃ at 5 ℃/min, and then increased to 180 ℃ at 20 ℃/min and maintained at 180 ℃ for 9 min, for a total of 30 min (8). Under a magnetic or electric field, the GC-MS transforms molecules into ions, separating the mass-to-charge ratio (m/z) in time and space with the assistance of a high vacuum, and providing the molecular weight, formula for the compound, and structure (8). The TD tube (1/4 inch × 7 inch, SEFM-G60200, Shanghai Amperex Scientific Instruments Co.) had a thin layer of chromatography silica gel H (Type 60) 0.2355 g (China Qingdao Ocean Chemical Group Corporation), which extracted the gas components into the sorbent packing. The TD tube was heated sequentially for 20 min (25 ℃ for 3 min before being increased to 265 ℃ at 200 ℃/min and maintained for 15.8 min), and then the extracted gas was volatilized by heat and released from the sorbent. Finally, qualitative and quantitative analyses were conducted using a GC-MS (8).

PEN

Rapid qualitative gas analysis was performed using the PEN3, which has 10 metal oxide sensor arrays, including W1C (aromatic benzenes), W5S (ammonia oxides), W3C (ammonia), W6S (hydrogen), W5C (alkanes), W1S (methane), W1W (hydrogen sulfide), W2S (ethanol), W2W (hydrogen sulfide), and W3S (aromatic alkanes) (9). The conductivity G of the sensors was modified in a sample containing volatiles. The concentration of each component in the sample was calculated using the G/G0 ratio of the 10 sensors with variable selectivity. The intensity of the sensor response value was then used for analysis, and was estimated as the concentration of each constituent in the sample (9).

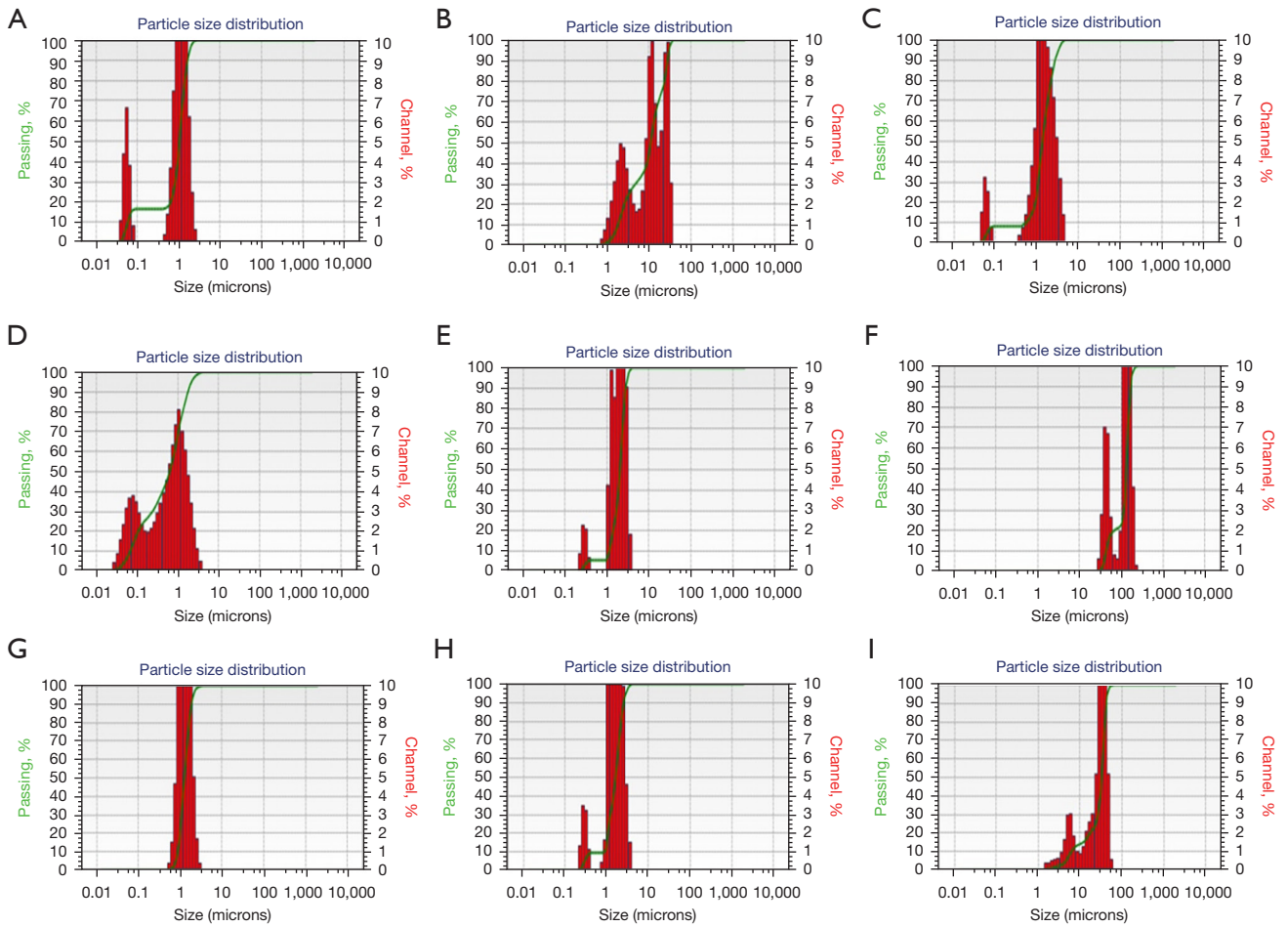

Figure 4 *In vitro* experiment particle size distribution of three electrosurgical devices on liver, skin, and muscle tissues. (A) Liver dissected by ES; (B) liver dissected by PB; (C) liver dissected by NTS-100; (D) skin dissected by ES; (E) skin dissected by PB; (F) skin dissected by NTS-100; (G) muscle dissected by ES; (H) muscle dissected by PB; (I) muscle dissected by NTS-100. ES, high frequency electrotome; PB, PlasmaBlade; NTS-100, new surgical system that applies low-temperature plasma.

Laser particle size analysis

The size distribution of solid particles in surgical smoke was examined using an LPSA. With an LSPA, articles in the sample are exposed to a laser beam to produce diffraction and an intensity distribution that is projected on the detector, which allows the light signal to be transformed into an electrical signal; the intensity is proportional to the particle diameter (10).

Statistical analysis

The experimental data were processed using SPSS 22.0 statistical software (IBM Corp. Released 2013. IBM SPSS Statistics for Windows, Version 22.0. Armonk, NY, USA: IBM Corp.) and expressed as the mean ± standard deviation. Comparisons of sample means between multiple groups were performed by one-way analysis of variance (ANOVA), with $P<0.05$ being statistically different and $P<0.01$ being statistically significantly different.

Results

Particle analysis

Particle size distribution

Particles collected in the gas collection bottle with 40 mL ultrapure water were analyzed by LPSA. *Figure 4* illustrates the size distribution by percentage passage and percentage channel for each of the cutting settings. *Table 1* displays the

Table 1 Average diameter of particles produced by nine different cutting conditions of *in vitro* experiment (μm), n=15

	ES	PB	NTS-100
Liver	0.988±0.690	12.692±3.325**	2.585±0.784**
Skin	0.775±0.382	2.507±0.277**	122.223±34.034**
Muscle	0.942±0.298	2.625±0.639**	29.192±6.518**

**, significant difference with the ES (P<0.01). Data were shown as mean ± SD. ES, electrotome; PB, PlasmaBlade; NTS-100, new surgical system that applies low-temperature plasma.

Table 2 Average concentration of PM2.5 produced by nine different cutting conditions of *in vivo* experiment (μg/m^3), n=3

	ES	PB	NTS-100
Liver	3,547.50±45.40	913.00±87.41**	924.67±79.22**
Skin	3,913.50±40.86	1,018.00±29.16**	1,079.00±81.68**
Muscle	3,742.25±42.25	1,534.33±61.06**	1,483.67±40.75**

**, significant difference with the ES (P<0.01). Data were shown as mean ± SD. ES, electrotome; PB, PlasmaBlade; NTS-100, new surgical system that applies low-temperature plasma.

Table 3 Average concentration of PM2.5 produced by nine different cutting conditions of *in vitro* experiment (μg/m^3), n=3

	ES	PB	NTS-100
Liver	4,124.50±91.25	1,192.00±53.37**	1,148.33±63.61**
Skin	4,200.25±68.72	2,203.67±97.19**	2,298.33±41.79**
Muscle	4,156.60±21.40	2,646.33±45.11**	2,757.33±62.90**

**, significant difference with the ES (P<0.01). Data were shown as mean ± SD. ES, electrotome; PB, PlasmaBlade; NTS-100, new surgical system that applies low-temperature plasma.

average diameter of particles in the samples. Applied to the same tissue, the NTS-100 produced aerosolized mist with considerably larger particles than did the PB and ES (P<0.05 and P<0.01, respectively). Specifically, the 122.223±34.034 μm mean diameter of NTS-100 particles (minimum diameter >10 μm) produced during skin tissue dissection was much larger than the 0.775±0.382 μm and 2.507±0.277 μm mean particle diameters with ES and PB, respectively. The mean diameter of NTS-100 particles produced during muscle tissue dissection was 29.192±6.518 μm (minimum diameter >1 μm), which was much larger than that of ES (0.942±0.298 μm) and PB (2.625±0.639 μm) particles. The mean diameter of NTS-100 particles produced during liver tissue dissection was 2.585±0.784 μm, which was a smaller particle diameter than with PB (12.692±3.325 μm) but larger particle diameter than with ES (0.988±0.690 μm).

Concentration of PM2.5

In vivo experiment

The average PM2.5 concentrations for the nine different cutting settings are shown in *Table 2*. The smoke observed during the operative procedure is shown in Figure S1. The real-time PM2.5 concentrations during the *in vivo* experiment were detected with the PM2.5 sensor positioned at the same height and distance from the incision for each cutting setting. The average PM2.5 concentration generated by the NTS-100 during muscle dissection (1,483.67±40.75 μg/m^3) was significantly higher than that generated during skin tissue dissection (1,079.00±81.68 μg/m^3) (P<0.05). Similarly, the PM2.5 concentration produced by the NTS-100 during skin tissue dissection was significantly higher than that produced during liver tissue dissection (924.67±79.22 μg/m^3). The concentration of PM2.5 generated by the PB during the cutting of muscle, skin, and liver decreased in that order, and the same order was observed with the NTS-100. With the ES, however, the PM2.5 concentration did not differ between the three tissue types (P>0.05). Furthermore, the PM2.5 concentrations produced by the NTS-100 were significantly lower than those produced by the ES (liver: 3,547.50±45.40 μg/m^3, skin: 3,913.50±40.86 μg/m^3, muscle: 3,742.25±42.25 μg/m^3) (P<0.05), but they did not differ significantly from those produced by the PB (liver: 913.00±87.41 μg/m^3, skin: 1,018.00±29.16 μg/m^3, muscle: 1,534.33±61.06 μg/m^3) (P>0.05).

In vitro experiment

Table 3 shows the average PM2.5 concentration for the PB, ES, and NTS-100. With the NTS-100, the PM2.5 concentration generated during muscle dissection (2,757.33±62.90 μg/m^3) was approximately 2.5-fold that generated during liver dissection (1,148.33±63.61 μg/m^3) (P<0.01), but no statistically significant difference was observed in PM2.5 concentration between skin tissue (2,298.33±41.79 μg/m^3) and liver or muscle tissue (P>0.05). In contrast, with the ES, there was no significant difference in the PM2.5 concentration between the three tissue types (P>0.05). Of note, the PM2.5 concentrations produced by the NTS-100 were significantly lower than those produced by the ES (liver: 4,124.50±91.25 μg/m^3, skin: 4,200.25±68.72 μg/m^3, muscle: 4,156.60±21.40 μg/m^3) (P<0.05) and were comparable to those produced by the PB (liver:

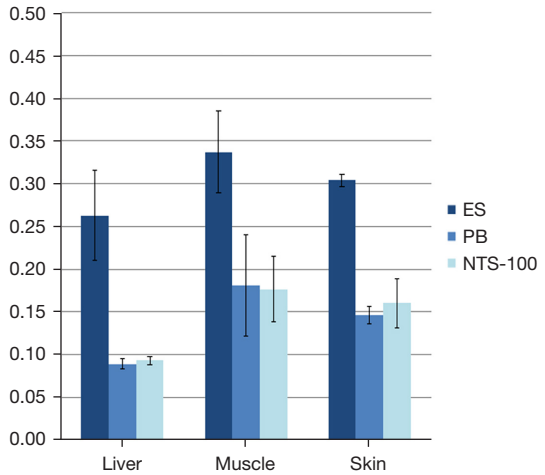

Figure 5 *In vitro* experiment particle mass of three electrosurgical devices on liver, skin, and muscle tissues. ES, electrotome; PB, PlasmaBlade; NTS-100, new surgical system that applies low-temperature plasma.

Table 4 Average particle mass produced by nine different cutting conditions of *in vitro* experiment (mg), n=30

	ES	PB	NTS-100
Liver	0.263±0.053	0.089±0.006**	0.093±0.004**
Skin	0.304±0.007	0.146±0.010*	0.160±0.004**
Muscle	0.337±0.048	0.181±0.059*	0.176±0.038**

*, significant difference with the ES (P<0.05); **, significant difference with the ES (P<0.01). Data were shown as mean ± SD. ES, electrotome; PB, PlasmaBlade; NTS-100, new surgical system that applies low-temperature plasma.

1,192.00±53.37 μg/m^3, skin: 2,203.67±97.19 μg/m^3, muscle: 2,646.33±45.11 μg/m^3) (P>0.05).

Mass of particle measurement

By weighing the particle filtering membranes (Figure S2), the mass of the particles was measured. *Figure 5* and *Table 4* show comparisons of particle mass between the ES, PB, and NTS-100. There was a significant difference between the mass of particles in surgical smoke generated by the NTS-100 during liver (0.093±0.004 mg), skin (0.160±0.004 mg), and muscle tissue dissection (0.176±0.038 mg). However, there was no statistically significant difference in the mass of particles produced when the ES was used to cut the three tissue types. Further, the NTS-100 generated significantly fewer particles than did the ES (liver: 0.263±0.053 mg, skin: 0.304±0.007 mg, muscle: 0.337±0.048 mg) (P<0.05), while no difference in particle mass was observed between the PB and the NTS-100 (liver: 0.089±0.006 mg, skin: 0.146±0.010 mg, muscle: 0.181±0.059 mg) (P>0.05).

Component analysis

PEN3

In vivo experiment

Table 5 and Figure S3 present the hazardous VOCs in surgical smoke produced by the different tools and tissue types. When the NTS-100 was used, there were only two hazardous components detected with all three tissue types: amino oxide (liver: 1.44±0.13, skin: 1.51±0.14, muscle: 2.35±0.21) and methane (liver: 1.44±0.23, skin: 1.43±0.17, muscle: 1.43±0.20). On the other hand, the ES generated aromatic amino oxide (liver: 3.67±0.09, skin: 2.60±0.09, muscle: 2.43±0.12), ammonia, hydrogen, alkane, methane (liver: 4.77±0.26, skin: 1.46±0.06, muscle: 2.73±0.26), organic sulfur, ethanol, and sulfur, while the PB generated amino oxide (liver: 1.31±0.28, skin: 1.47±0.11, muscle: 1.31±0.23), hydrogen, methane (liver: 2.43±0.06, skin: 2.30±0.21, muscle: 2.25±0.14), ethanol, and sulfur. Therefore, the smoke produced by the NTS-100 contained far fewer hazardous components than that produced by the ES and PB.

In vitro experiment

Table 6 and Figure S4 show the results of surgical smoke analysis by PEN3 in the sealed glass bottle. Surgical smoke produced by the NTS-100 contained lower concentrations of harmful components than smoke produced by the ES (P<0.05) and showed no difference from smoke produced by the PB (P>0.05). Notably, only two compounds were detected during muscle tissue dissection with the NTS-100 (amino oxide: 1.63±0.06 and methane: 1.44±0.23), the concentrations of which were both significantly lower than they were with the ES (amino oxide: 2.64±0.15 and methane: 3.88±0.19), and no significant difference was observed between the ES and the PB (amino oxide: 3.54±0.14 and methane: 2.44±0.11). Moreover, the concentration of aromatic benzene was lower with the NTS-100 (liver: 1.21±0.25, skin: 1.23±0.12, muscle: NA) than with the PB (liver: 1.33±0.11, skin: 1.55±0.16, muscle: 1.46±0.23) and the ES (liver: 1.72±0.04, skin: 2.81±0.22, muscle: 1.68±0.33).

In vitro GC-MS results

Table 7 shows the smoke composition and volume concentration evaluated by GC-MS. Under all the cutting conditions, muscle tissue produced more types of chemical

Table 5 Smoke composition and sensor response intensity produced by nine cutting conditions of *in vivo* experiment (G/G0), n=3

Chemical compounds	Liver			Skin			Muscle		
	ES	PB	NTS-100	ES	PB	NTS-100	ES	PB	NTS-100
Aromatic	1.73±0.24	–	–	1.44±0.12	1.31±0.06	–	1.57±0.25	–	–
Amino oxide	3.67±0.09	1.31±0.28**	1.44±0.13**	2.60±0.09	1.47±0.11**	1.51±0.14**	2.43±0.12	1.31±0.23	2.35±0.21
Ammonia	1.66±0.31	–	–	1.46±0.24	–	–	1.56±0.09	–	–
Hydrogen	2.68±0.11	1.36±0.12**	–	2.65±0.11	–	–	1.77±0.21	2.10±0.32	–
Alkane	1.68±0.32	–	–	1.57±0.19	1.33±0.05	–	1.51±0.17	–	–
Methane	4.77±0.26	2.43±0.06**	1.44±0.23**	1.46±0.06	2.30±0.21	1.43±0.17	2.73±0.26	2.25±0.14	1.43±0.20
Organic sulfur	2.68±0.18	–	–	2.84±0.34	1.36±0.13*	–	2.80±0.21	–	–
Ethanol	2.71±0.14	1.33±0.22**	–	1.61±0.13	1.33±0.21	–	1.62±0.11	1.46±0.18	–
Sulphur	2.52±0.31	1.35±0.10*	–	2.84±0.08	1.37±0.12**	–	2.74±0.34	1.35±0.23	–

*, significant difference with the ES (P<0.05); **, significant difference with the ES (P<0.01). Data were shown as mean ± SD. ES, electrotome; PB, PlasmaBlade; NTS-100, new surgical system that applies low-temperature plasma.

Table 6 Smoke composition and sensor response intensity produced by nine cutting conditions of *in vitro* experiment (G/G0), n=3

Chemical compounds	Liver			Skin			Muscle		
	ES	PB	NTS-100	ES	PB	NTS-100	ES	PB	NTS-100
Aromatic	1.72±0.04	1.33±0.11	1.21±0.25	2.81±0.22	1.55±0.16	1.23±0.12	1.68±0.33	1.46±0.23	–
Amino oxide	5.68±0.12	4.21±0.34	2.43±0.11*	5.04±0.18	6.20±0.36	1.92±0.11**	2.64±0.15	3.54±0.14	1.63±0.06*
Ammonia	1.77±0.33	1.28±0.46	1.38±0.06	2.80±0.13	1.34±0.21	1.53±0.26	1.56±0.41	1.52±0.22	–
Hydrogen	2.93±0.10	3.49±0.03	2.82±0.21	7.84±0.09	1.44±0.13**	–	3.68±0.07	–	–
Alkane	2.42±0.43	1.02±0.22*	1.15±0.17*	2.33±0.23	1.21±0.16*	1.47±0.12*	1.53±0.25	1.66±0.09	–
Methane	4.87±0.11	2.19±0.13**	2.64±0.09**	6.73±0.11	3.57±0.26**	2.38±0.10**	3.88±0.19	2.44±0.11	1.44±0.23**
Organic sulfur	2.31±0.03	2.66±0.41	2.29±0.15	5.28±0.10	1.78±0.18**	2.77±0.25**	3.63±0.26	2.61±0.32	–
Ethanol	4.76±0.09	1.42±0.06**	2.01±0.63**	4.21±0.13	2.41±0.09**	1.55±0.26**	2.59±0.21	2.43±0.15	–
Sulphur	3.52±0.21	2.28±0.04*	2.45±0.12*	6.28±0.04	2.82±0.12**	1.87±0.24**	3.84±0.11	1.29±0.24**	–
Aromatic alkanes	–	–	–	1.44±0.22	–	–	–	–	–

*, significant difference with the ES (P<0.05); **, significant difference with the ES (P<0.01). Data were shown as mean ± SD. ES, electrotome; PB, PlasmaBlade; NTS-100, new surgical system that applies low-temperature plasma.

components than did skin or liver tissue. In particular, using the NTS-100, muscle tissue generated hydrocarbons and aldehydes while skin tissue did not, and generated alcohols, sulfides, and aldehydes while liver tissue did not. In comparison with the PB and ES, the NTS-100 generated fewer harmful components and produced a lower concentration of surgical smoke than did the ES (P<0.05), but showed no discernible differences from the PB (P>0.05). In particular, the concentrations of aromatics produced by the NTS-100 (liver: 8.74%±1.36%, skin: 7.15%±1.83%, muscle: 5.04%±0.88%) were much lower than those produced by the ES (liver: 21.12%±2.38%, skin: 18.07%±4.47%, muscle: 15.66%±2.42%) (P<0.05), and lower than those produced by the PB (liver: 10.36%±2.41%, skin: 9.54%±2.66%, muscle: 10.03%±1.34%) (P>0.05) in all experiments.

Table 7 Smoke composition and volume concentration produced by nine different cutting conditions of *in vitro* experiment (%), n=3

Chemical compounds	Liver			Skin			Muscle		
	ES	PB	NTS-100	ES	PB	NTS-100	ES	PB	NTS-100
Water	37.39±4.28	47.89±1.01	48.71±0.97	45.10±4.92	46.80±3.08	48.68±3.81	41.18±4.87	41.87±5.76	45.56±3.01
Ammonia	10.52±2.33	11.01±0.29	11.01±0.29	11.22±2.81	11.74±1.19	11.64±2.39	20.11±3.27	15.64±2.70**	16.20±1.25*
Carbon dioxide	13.80±4.51	30.44±0.46	30.53±0.75	15.09±2.13	30.33±0.31	30.26±5.34	13.79±1.46	31.25±2.44	29.02±3.21
Aromatics	21.12±2.38	10.36±2.41**	8.74±1.36**	18.07±4.47	9.54±2.66**	7.15±1.83**	15.66±2.42	10.03±1.34**	5.04±0.88**
Hydrocarbons	9.88±3.66	0.39±0.01**	0.28±0.10**	6.31±1.22	3.46±0.19**	–	6.86±0.21	3.41±0.18**	3.52±0.11**
Alcohols	3.76±0.28	1.21±0.21**	–	1.97±0.08	–	0.39±0.14**	4.89±0.92	1.92±0.17**	0.71±0.13**
Ketones	0.61±0.13	–	–	4.11±0.33	–	–	0.20±0.03	–	–
Amines	1.40±0.20	–	0.74±0.09**	1.58±0.11	–	2.76±0.19*	0.85±0.10	0.71±0.23	3.53±0.31**
Amino acids	0.74±0.09	–	–	–	–	–	0.06±0.02	–	–
Sulfides	–	–	–	0.51±0.03	–	0.05±0.01**	0.60±0.03	0.08±0.01**	0.08±0.02**
Nitriles	–	–	–	0.37±0.04	–	–	1.43±0.18	–	–
Aldehydes	–	–	–	–	–	–	2.35±0.22	–	1.32±0.12*

*, significant difference with the ES (P<0.05); **, significant difference with the ES (P<0.01). Data were shown as mean ± SD. ES, electrotome; PB, PlasmaBlade; NTS-100, new surgical system that applies low-temperature plasma.

Discussion

In this study, the NTS-100 generally produced less harmful surgical smoke than did the ES and was comparable to the PB in terms of the types and concentrations of VOCs, PM2.5 concentrations, and the mass of particles. Remarkably, the NTS-100 generated larger particles than did the ES and PB.

As shown in *Figure 3*, to ensure precision and accuracy for the *in vitro* experiment, we specially designed an entirely enclosed system for smoke generation, collection, measurement, and analysis. In addition to the fully enclosed tissue dissection and smoke transportation procedure, the initial air was evacuated from the container before the experiment by flushing with helium. To our knowledge, most of the surgical smoke collection devices used in previous studies can be broadly classified into two types according to the purpose of the research: first, to measure operating room personnel's exposure to surgical smoke by measuring at levels approximating respiratory zone (11,12). Second, the researches aimed to evaluate the chemical compounds and PMs generated in different cutting conditions (i.e., different tissues, different electrosurgical devices, and difference between endoscopic surgery and thoracotomy) would collect all generated smoke as much as possible. Previous studies have used conductive tubes and an electrostatic precipitation collection device that uses the force of an induced electrostatic charge to minimize particle electrical losses (13,14). As with any surgical collection system stated in prior research, some particles may escape naturally away from these inlet areas and not be collected (11-14). Considering the aim of this research was to compare the surgical smoke generated during electrosurgery with hazardous composition from the ES, the comparative PB and the NTS-100, the surgical analysis system was designed to avoid the escape of the smoke. Similarly, *in vivo* experiment, the gas collecting tube was tightly attached to the scalpel tip. Also, unlike a previous analysis of surgical smoke from porcine tissues that used electrical low-pressure impactor analysis with an upper range of 10 μm, we used LPSA (range, 0.02–2,800 μm) to avoid underestimating the particle size (14). Furthermore, we conducted experiments on anesthetized healthy swine for physiological mimicry of the actual surgical procedure, whereas the majority of reported studies used only fresh tissues (13-16).

The results of this research reconfirm the smoke hazard of the ES. In total, ten types of VOCs were detected, including benzene, methane, and organic sulfur, which are known carcinogens. The average particle diameter was <1 μm. These findings emphasize the importance of technically advanced electrocautery. The PB uses pulsating

radio frequency to generate a thin layer of plasma containing accelerated electriferous particles (4,5) that cut the link between each cell to realize cutting and dispelling (4,5). This technique decreases the energy required as well as burn on tissues. Further, the NTS-100 has a lower tip temperature than the PB.

The types of VOCs detected in this study were similar to those reported in previous studies, but the results for PM differed (11,12,14,15). According to Karjalainen *et al.* (14), the liver is a high-PM tissue, muscle is a medium-PM tissue, and skin is a low-PM tissue; however, in the present study, no noticeable difference was observed between these tissues in surgical smoke generated by the ES. Our findings are supported by other research. For example, Hinz *et al.* (17) and Casey *et al.* (13) reported similar particle size distribution for the different tissues. It is noteworthy that the particle size distribution for liver tissue in this research was similar to that of Casey *et al.* (13), with >90% of the particles detected with the ES during liver tissue dissection being classified as PM2.5. The varying results of these studies may be explained by the different experimental and measurement systems used (13,14,17). Karjalainen *et al.* (14) calculated mass depositions in airways, whereas we measured the mass and concentration of the total generated smoke, which was a more comprehensive measurement.

Overall, the NTS-100 generated larger particles than did the PB or the ES (*Table 1*). It also generated fewer particles than did the ES but showed no significant difference with the PB (*Tables 2-4*). The size of the particles in surgical smoke is important. Particles can be classified as coarse (2.5–10 μm), fine (0.1–2.5 μm), or ultrafine (<0.1 μm), with the degree of toxicity being greater in smaller particles (18,19). Particles with a diameter <10 μm (PM10) can be inhaled (19). When the NTS-100 was used to cut skin and muscle tissue, the average particle diameters were >10 μm (122.223±34.034 and 29.192±6.518 μm, respectively), which was significantly larger than the average particle diameters with the PB (2.507±0.277 and 2.625±0.639 μm, respectively) and the ES (0.775±0.382 and 0.942±0.298 μm, respectively). In addition, particles with a diameter <2.5 μm can absorb VOCs, such as polycyclic aromatic hydrocarbons and benzene, as well as heavy metals (3,20). When the NTS-100 was used to cut liver tissue, the average particle diameter was 2.585±0.784 μm, which was significantly larger than that for particles generated by the ES (0.988±0.690 μm). Furthermore, ultrafine particles are capable of penetrating cells (20,21). For all experimental tissue types, the average diameter of particles with the ES was <1 μm, with a certain proportion of particles being <0.1 μm. In comparison, the NTS-100 generated particles >1 μm when cutting skin and muscle tissues. We speculate that this result could be related to the fact that the working temperature of the NTS-100 (average tip temperature during cutting ~70 ℃) is lower than that of the PB (~80 ℃). However, further study is needed to investigate this point.

The surgical smoke generated by the NTS-100 had fewer detectable types and lower concentrations of VOCs compared to smoke produced by the ES, while showing no significant differences with the smoke produced by PB. It should be noted that the NTS-100 demonstrated an excellent performance in the *in vivo* experiment and released a lower concentration of benzene in all experiments. Despite the chemical composition of surgical smoke varying with the type of surgery, instruments, and tissues, several hazardous toxins have been consistently detected (3,11,12,15). Most of the compounds detected in this research are classified as hazardous to human health when exceeding the recommended limits (3). In this study, the proportion of aromatic compounds ranked high among all chemical compounds. Notably, the NTS-100 generated fewer aromatic chemical compounds than did the ES and PB in all experiments. We speculate that the lower tip temperature of the NTS-100 may explain this finding. Unfortunately, due to the limitations of the detection instruments, only qualitative and relatively quantitative VOCs analyses were conducted in this research, and our results cannot be referenced to security standards or data from previous research.

Interestingly, in the *in vivo* experiments, the NTS-100 generated fewer types and lower concentrations of VOCs than did the PB, whereas the VOCs types and concentrations generated by the PB and the NTS-100 were similar in the *in vitro* experiment. In the *in vivo* experiment, the NTS-100 only generated ammonia oxides and methane while cutting the different tissues, which might be a result of the *in vivo* blood supply affecting the types and concentrations of VOCs. Consequently, it is assumed that the NTS-100 will perform effectively in clinic. However, the possibility of escaping smoke undermines the conclusions of the *in vivo* experiments, and additional studies are required in the future.

The NTS-100 was superior to the ES and the PB for cutting muscle tissues. The ES did not show statistically significant differences in terms of chemical compounds or PM in the surgical smoke for any of the three tissues in this study. Conversely, the NTS-100 and PB yielded similar results to each other, with the amounts and concentrations of

particles being highest for muscle tissue followed by skin and subcutaneous tissue, and lowest for liver tissue. Considering this, escalation from the ES to the PB and the NTS-100 seems to be less effective for muscle tissue than for liver or skin tissue at the particle level. However, as shown in *Table 1*, during muscle tissue dissection, the NTS-100 generated larger particles than did the PB (average particle size 29.192±6.518 μm and 0.942±0.298 μm, respectively), and the minimum particle diameter distribution with the NTS-100 was >1 μm. In other words, the NTS-100 minimizes the likelihood of particles in surgical smoke being inhaled.

This study has some limitations. First, the ventilation of the room and the baseline levels of PM and VOCs and before each *in vivo* experiment were not measured. Second, electrosurgery is challenging to standardize, which can lead to inaccuracies. Third, this study was conducted purely in experimental animals, whose tissues differ from those of humans. Further, there was possible biological variability resulting from the limited number of animals. Finally, more studies are needed to ascertain whether there is a risk of COVID-19 transmission during NTS-100 operation.

The PB is reported to perform better than the ES in terms of wound healing and duration time for procedures such as tonsillectomy, breast reconstruction, the replacement of implanted medical devices, and surgical debridement of chronic ulcers (4,22,23). Previous research has also confirmed that the NTS-100 is superior to the most developed PB in terms of the number of tissue injuries and its cutting and coagulating capability (24), and the NTS-100 has already been used effectively in breast, head and neck, and general surgery. Our findings illustrate that the NTS-100 generated substantially less hazardous surgical smoke than did the PB or the ES. We therefore consider the NTS-100 to have a promising future, although data from further clinical comparisons with existing electrosurgical devices are still needed to improve our system.

Conclusions

Hazardous chemical compounds and PM were detected in surgical smoke produced by the conventional ES, the comparative PB, and the NTS-100. Surgical smoke produced by the NTS-100 contained fewer hazardous components than that produced by the ES. However, the NTS-100 and PB were generally indistinguishable from each other in terms of the harmful components detected. Therefore, the NTS-100 may be a promising way to reduce the potential hazard posed by surgical smoke to operating room personnel.

Acknowledgments

Funding: This work was supported by Translational Medicine Project of PLA General Hospital (grant No. 2016TM-006).

Footnote

Reporting Checklist: The authors have completed the ARRIVE reporting checklist. Available at https://atm.amegroups.com/article/view/10.21037/atm-22-608/rc

Data Sharing Statement: Available at https://atm.amegroups.com/article/view/10.21037/atm-22-608/dss

Peer Review File: Available at https://atm.amegroups.com/article/view/10.21037/atm-22-608/prf

Conflicts of Interest: All authors have completed the ICMJE uniform disclosure form (available at https://atm.amegroups.com/article/view/10.21037/atm-22-608/coif). The authors have no conflicts of interest to declare.

Ethical Statement: The authors are accountable for all aspects of the work in ensuring that questions related to the accuracy or integrity of any part of the work are appropriately investigated and resolved. Experiments were performed under a project license (No. 20160010703) granted by the Ethics Committee of Chinese PLA General Hospital, in compliance with the NIH guidelines for the care and use of animals.

References

1. Zakka K, Erridge S, Chidambaram S, et al. Electrocautery, Diathermy, and Surgical Energy Devices: Are Surgical Teams at Risk During the COVID-19 Pandemic? Ann Surg 2020;272:e257-62.

2. Cheruiyot I, Sehmi P, Ngure B, et al. Laparoscopic surgery during the COVID-19 pandemic: detection of SARS-COV-2 in abdominal tissues, fluids, and surgical smoke. Langenbecks Arch Surg 2021;406:1007-14.
3. Limchantra IV, Fong Y, Melstrom KA. Surgical Smoke Exposure in Operating Room Personnel: A Review. JAMA Surg 2019;154:960-7.
4. Peprah K, Spry C. Pulsed Electron Avalanche Knife (PEAK) PlasmaBlade versus Traditional Electrocautery for Surgery: A Review of Clinical Effectiveness and Cost-Effectiveness. Ottawa (ON): Canadian Agency for Drugs and Technologies in Health; August 9, 2019.
5. Kisch T, Liodaki E, Kraemer R, et al. Electrocautery Devices With Feedback Mode and Teflon-Coated Blades Create Less Surgical Smoke for a Quality Improvement in the Operating Theater. Medicine (Baltimore) 2015;94:e1104.
6. Pang L, Zhang H, Yang G. Application of Chinese Bama minipigs in medical research: a literature review. Acta Laboratorium Animalis Scientia Sinica 2014;22:94-8.
7. Hu J. comparative biological research of skin in BAMA minipig. Chongqing: Southwest University, 2006.
8. Cai D. Application of gas chromatography-mass spectrometry in food inspection. Biotech World 2015(01):10.
9. Jiang L, Pan L, Tu K, et al. Freshness Evaluation of Juicy Peach by Electronic Nose. Food Science 2010;31:229-32.
10. Yang D, Ma C, Sun H, et al. Research on Particle Size Determination Method and Optimization of Malvern Lazer Particle Analyzer, China Powder Science and Technology 2002;8:27-30.
11. Ha HI, Choi MC, Jung SG, et al. Chemicals in Surgical Smoke and the Efficiency of Built-in-Filter Ports. JSLS 2019;23:e2019.
12. Cheng MH, Chiu CH, Chen CT, et al. Sources and components of volatile organic compounds in breast surgery operating rooms. Ecotoxicol Environ Saf 2021;209:111855.
13. Casey VJ, Martin C, Curtin P, et al. Comparison of Surgical Smoke Generated During Electrosurgery with Aerosolized Particulates from Ultrasonic and High-Speed Cutting. Ann Biomed Eng 2021;49:560-72.
14. Karjalainen M, Kontunen A, Saari S, et al. The characterization of surgical smoke from various tissues and its implications for occupational safety. PLoS One 2018;13:e0195274.
15. Markowska M, Krajewski A, Maciejewska D, et al. Qualitative analysis of surgical smoke produced during burn operations. Burns 2020;46:1356-64.
16. Kondo A, Watanabe Y, Ishida M, et al. Particle Size Distributions in Surgical Smoke Generated by Advanced Energy Devices: A Meaningful Perspective From an Experimental Study in the Time of COVID-19. Ann Surg 2021;273:e168-70.
17. Hinz KP, Gelhausen E, Schäfer KC, et al. Characterization of surgical aerosols by the compact single-particle mass spectrometer LAMPAS 3. Anal Bioanal Chem 2011;401:3165-72.
18. Espitia-Pérez L, Jiménez-Vidal L, Espitia-Pérez P. Particulate Matter Exposure: Genomic Instability, Disease, and Cancer Risk. In: Makan A. Environmental Health - Management and Prevention Practices. London: IntechOpen; 2020. Available online: https://www.intechopen.com/books/6877
19. Turner MC, Andersen ZJ, Baccarelli A, et al. Outdoor air pollution and cancer: An overview of the current evidence and public health recommendations. CA Cancer J Clin 2020. [Epub ahead of print]. doi: 10.3322/caac.21632.
20. Bae HR, Chandy M, Aguilera J, et al. Adverse effects of air pollution-derived fine particulate matter on cardiovascular homeostasis and disease. Trends Cardiovasc Med 2021. [Epub ahead of print]. pii: S1050-1738(21)00116-X. doi: 10.1016/j.tcm.2021.09.010.
21. Riediker M, Zink D, Kreyling W, et al. Particle toxicology and health - where are we? Part Fibre Toxicol 2019;16:19.
22. Chow WTH, Oni G, Ramakrishnan VV, et al. The use of plasmakinetic cautery compared to conventional electrocautery for dissection of abdominal free flap for breast reconstruction: single-centre, randomized controlled study. Gland Surg 2019;8:242-8.
23. Mittal S, Wilkoff BL, Poole JE, et al. Low-temperature electrocautery reduces adverse effects from secondary cardiac implantable electronic device procedures: Insights from the WRAP-IT trial. Heart Rhythm 2021;18:1142-50.
24. Zhong Y, Wei Y, Min N, et al. Comparative healing of swine skin following incisions with different surgical devices. Ann Transl Med 2021;9:1514.

Cite this article as: Zhang B, Guan Q, Zhu Y, Zhu J, Liu X, Li S, Yang R, Li X. Smoke analysis of a new surgical system that applies low-temperature plasma. Ann Transl Med 2022;10(19):1053. doi: 10.21037/atm-22-608

